Supplementary Materials

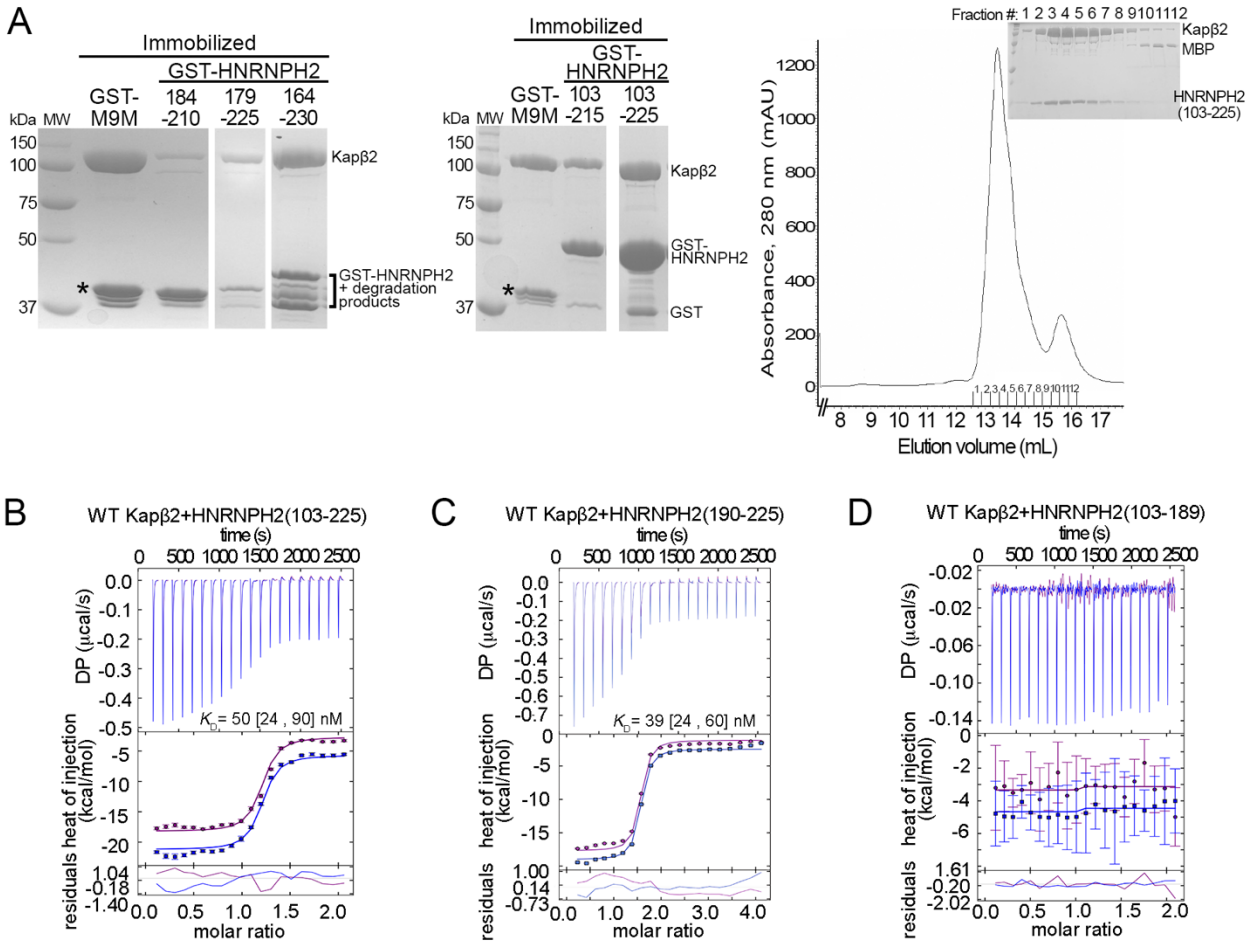

Figure S1. Identifying a stable HNRNPH2 fragment for optimal Kapβ2 interaction, related to Figure 1 and Table 1. (A) Left and middle panels: Pull-down binding assay of Kapβ2 with immobilized GST-HNRNPH2 constructs (on glutathione beads) of different lengths. Beads incubated with Kapβ2 were washed extensively before bound proteins were visualized by SDS-PAGE and Coomassie staining. Asterisks (*) label the immobilized positive control GST-M9M. GST-HNRNPH2(184-210) pulls down very little Kapβ2, GST-HNRNPH2(179-225) does not express well and the bracket indicates degraded GST-HNRNPH2(164-230). GST-HNRNPH2(103-225) in the last lane of the middle panel shows minimal degradation and binds well to Kapβ2. Right panel, size exclusion chromatography of a mixture of Kapβ2 and HNRNPH2(103-225), showing stable interaction of the two proteins. The MBP is from the cleavage of His_6-MBP-HNRNPH2(103-225) with Tev protease. **(B-D)** ITC analysis of Kapβ2 binding to MBP-HNRNPH2 fragments. Top panels show the reconstructed thermograms from NITPIC, middle panels show the binding isotherms and individual fits and bottom panels show fitting residuals. Dissociation constants (K_Ds) obtained from global analysis of duplicate measurements are displayed with 95% confidence intervals in brackets. For (**D**), no binding can be observed.

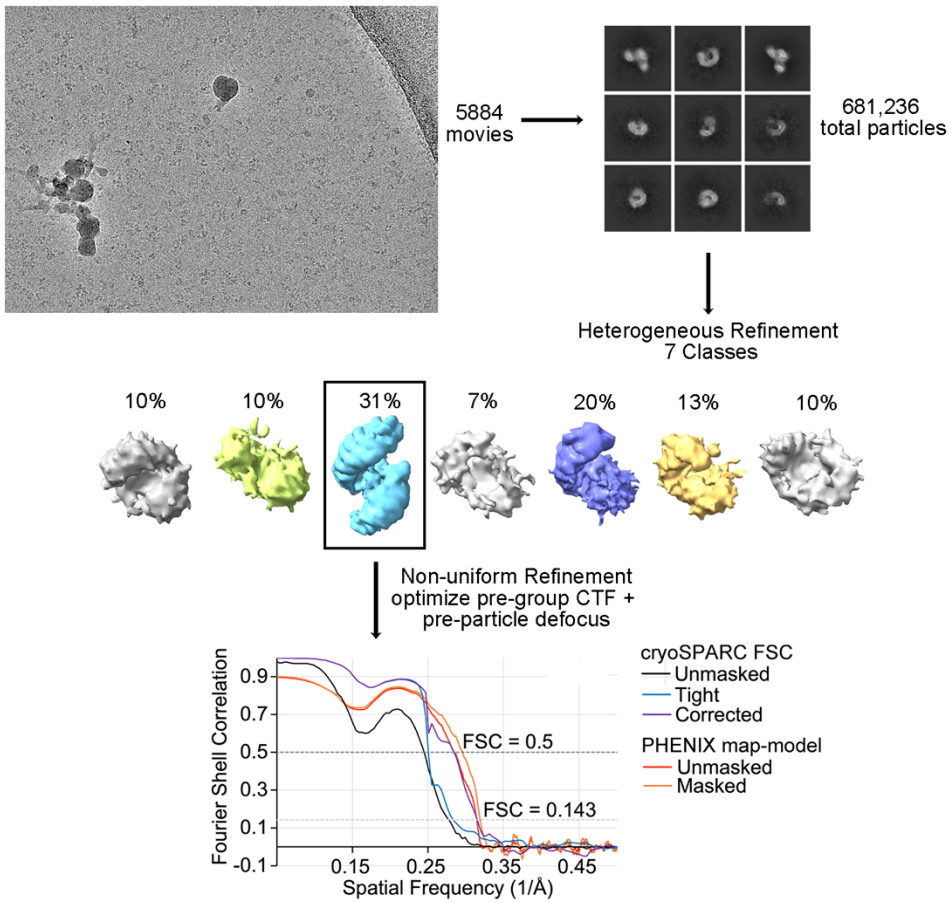

Figure S2. Cryo-EM structure determination of Kapβ2•HNRNPH2(103-225), related to Figure 1. 5884 movies were processed and 681,236 total particles (9 representative 2D templates are shown) were selected for 3D classification. Particles were classified into 7 classes using Heterogenous Refinement. The most populated class has the best-looking map (light blue), which was used for Non-uniform Refinement to obtain the final map. The rest of the classes appear to be junk particles (gray) or incomplete/poorly aligned Kapβ2 particles (other colors). FSC curves for final map from cryoSPARC (unmasked in black, tight/corrected mask in blue/purple) and map-model FSC from PHENIX (unmasked/masked in red/orange) were displayed.

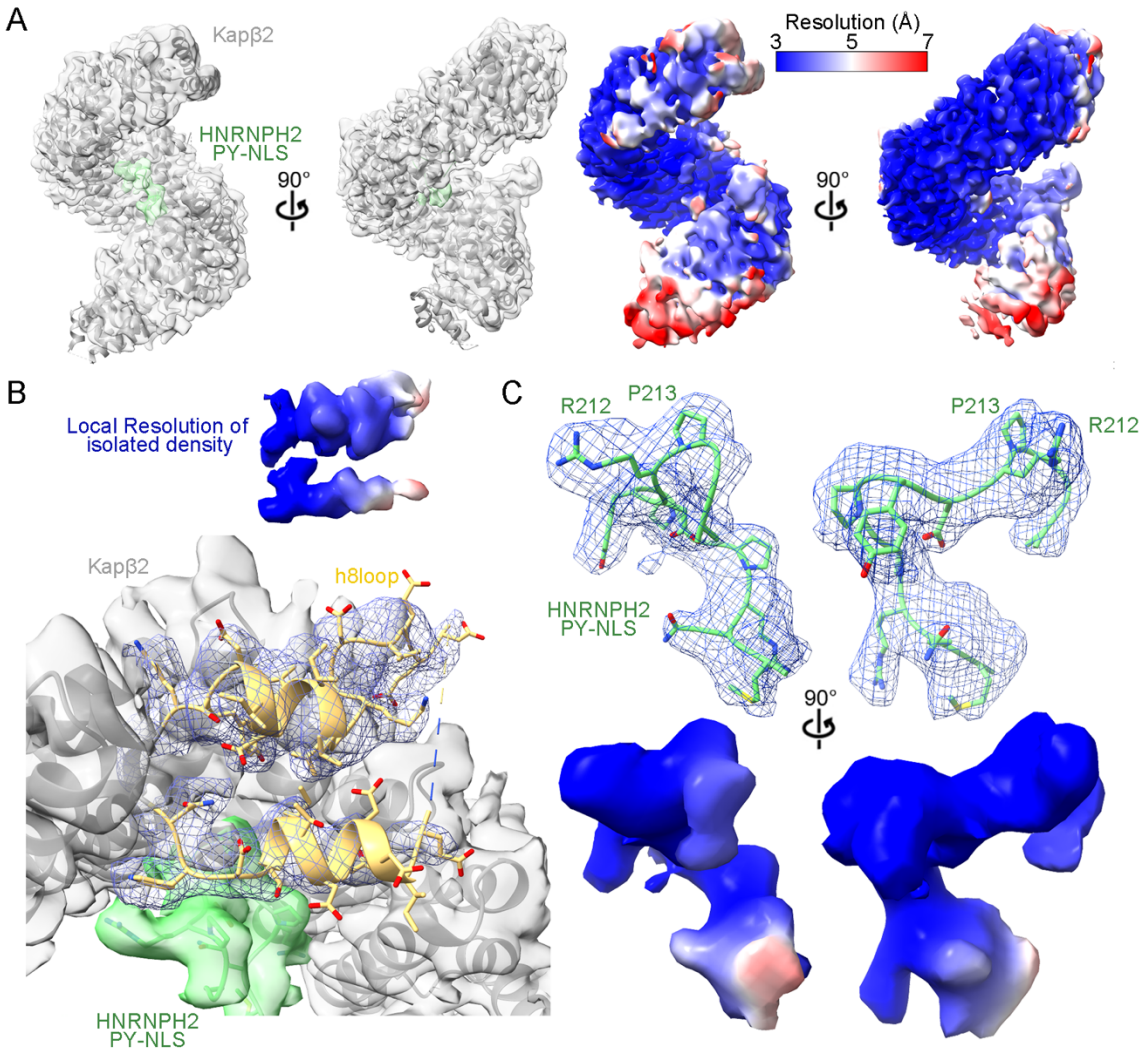

Figure S3. Map densities and local map resolution for Kapβ2•HNRNPH2(103-225), related to Figure 1. (A) The Kapβ2•HNRNPH2 model docked into the final map, colored gray for Kapβ2 and green for HNRNPH2. The same map is colored according to local resolution on the right. **(B-C)** Isolated map density (blue mesh) for the h8loop (yellow cartoon) **(B)** and the PY-NLS **(C)** and their corresponding local resolution.

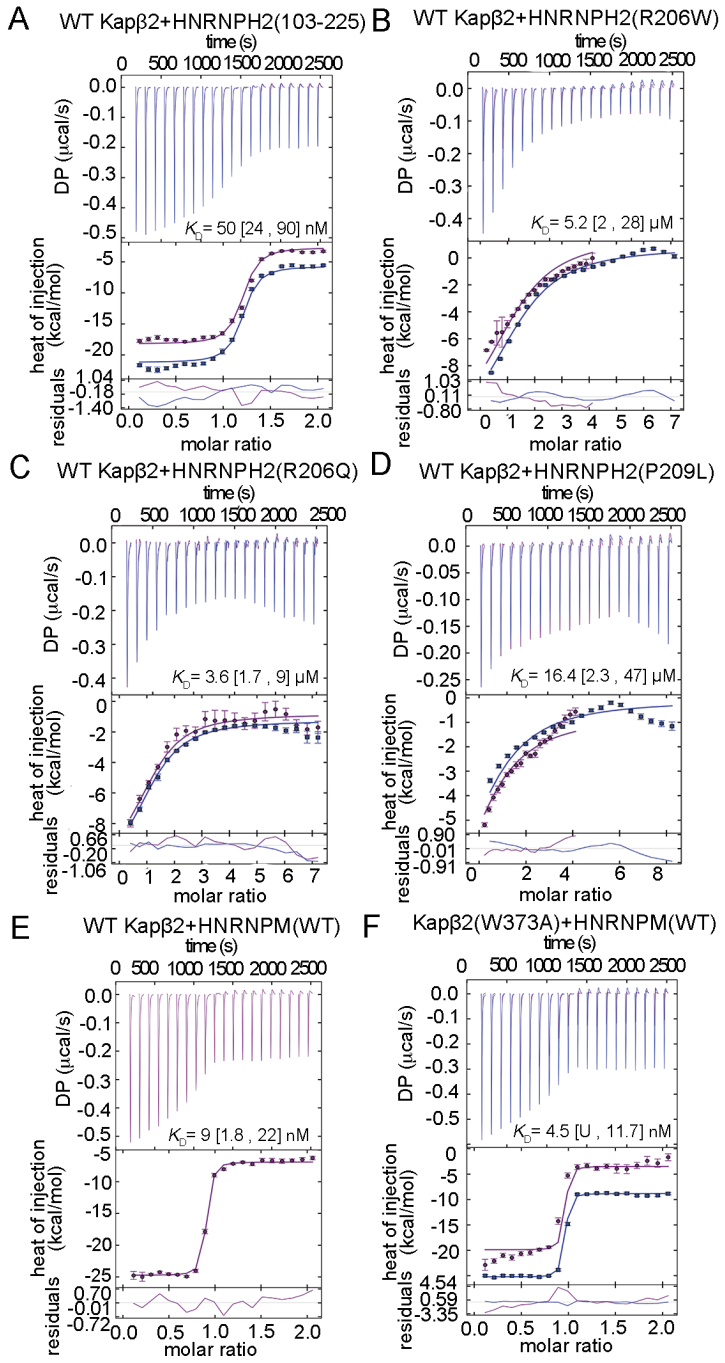

Figure S4. Mutagenesis analysis of Kapβ2 binding to HNRNPH2 and HNRNPM PY-NLSs by ITC, related to Figure 1 and Table 1. (A-D) ITC titrations of MBP-HNRNPH2(130-225) with indicated mutations into Kapβ2 WT. (A) is the same data with MBP-HNRNPH2(130-225) WT as Figure S1B, repeated here for comparison with MBP-HNRNPH2(130-225) mutants. Top panels illustrate the reconstructed thermograms from NITPIC, middle panels show the binding isotherm and individual fits, fitting residuals are plotted below. K_Ds obtained from global analysis of duplicate measurement are displayed with 95% confidence intervals in brackets. **(E-F)** As in **(A-D)**, but MBP-HNRNPM PY-NLS were titrated into WT Kapβ2 **(E)** and Kapβ2(W373A) **(F)**. U - unable to be determined. The K_D in **(F)** was obtained from global analysis of duplicate measurement and the K_D in **(E)** from a single experiment, which matches the previously reported K_D for the same WT Kapβ2 and MBP-HNRNPM PY-NLS constructs.[1]

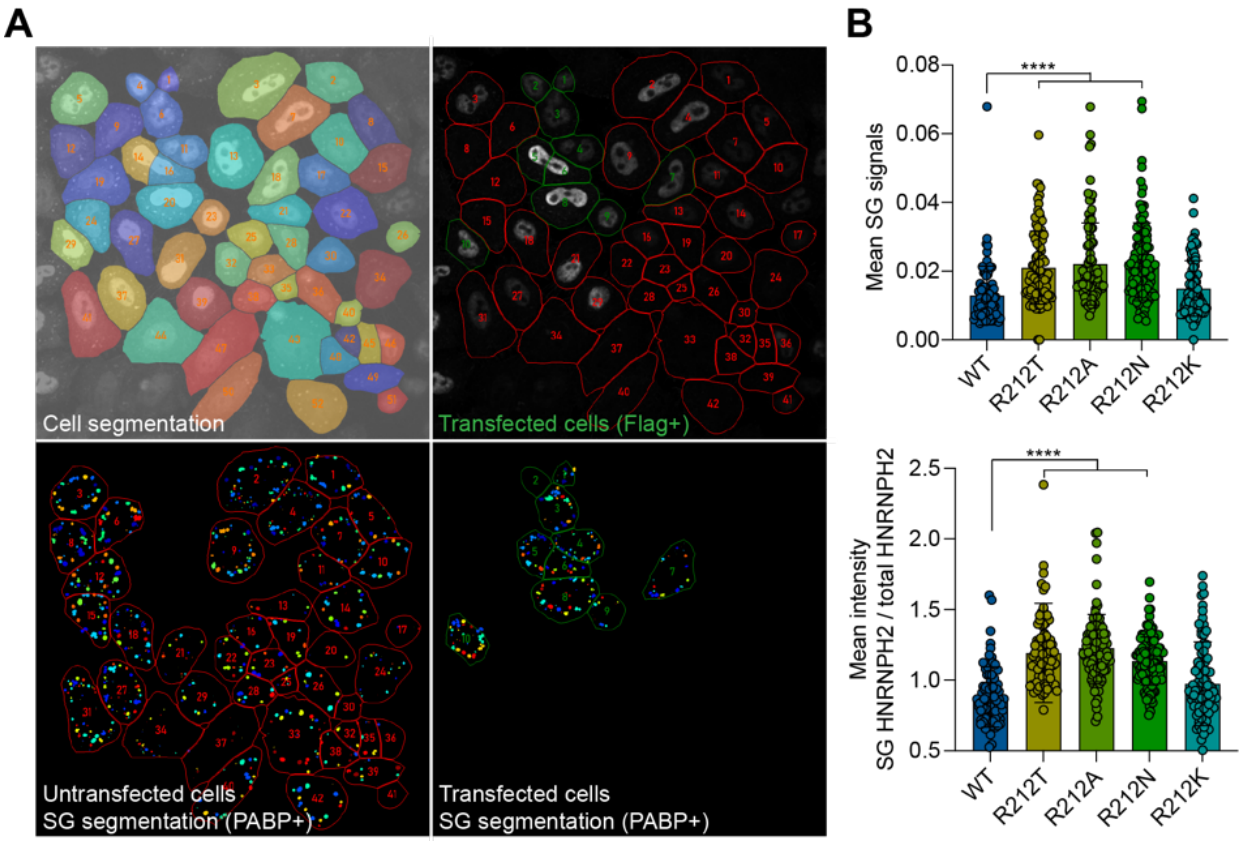

Figure S5. Automated puncta detection analysis for measuring stress granule association, related to Figure 3. (A) An example of data filtering and analysis using CellProfiler pipeline. The top left image shows a preview of cell segmentation with the total cell count, where only cells touching the edges were removed. The top right image displays the FLAG-stained cells, with their respective index numbers, where untransfected cells are overlaid with red and transfected cells with green. The bottom left and right images show stress granules detected in each untransfected and transfected cell, respectively. **(B)** Mean HNRNPH2 signal of all stress granules (top) and integrated HNRNPH2 signals of stress granules normalized to integrated signals of total HNRNPH2. The graphs represent the mean ± S.D. ****P<0.0001 by one-way ANOVA Dunnett's multiple comparison's test.

Table S1. Primers used in this study, related to STAR Methods.

Name	Primer Sequence
For HNRNPH2 fragments	
184 Forward (BamHI)	GCGGATCCTTCAAGAGTAGCCGAGCTGAAG
210 Reverse (Xho1)	GCAGCTCGAGTTAATAGGGACCTGGCCGCTG
179 Forward (BamHI)	GGCGGATCCAGGTACATTGAGATCTTCAAGAGTAG
225 Reverse (Xho1)	GCAGCTCGAGTTATCCTCTGCCAATGCTATTATAC
164 Forward (BamHI)	GCGGATCCATAGCTGAGAAGGCCTTAAAG
230 Reverse (Xho1)	CAGCTCGAGTTACCTTTCAAACCCAGCTC
103 Forward (BamHI)	GCGGATCCAATAGCCCTGATACTGCCAACG
215 Reverse (Xho1)	GCAGCTCGAGTTAAGCCCCCGGCCTATCATAG
189 Reverse (Xho1)	CAGCTCGAGTTAAGCTCGGCTACTCTTGAAG
For pHis-Mal-tev-HNRNPH2 mutants	
R212K Forward	AGGTCCCTATGATAAGCCGGGGGCTGGCA
R212K Reverse	TGCCAGCCCCCGGCTTATCATAGGGACCT
R212A Forward	AGGTCCCTATGATGCGCCGGGGGCTGGCA
R212A Reverse	TGCCAGCCCCCGGCGCATCATAGGGACCT
For pcDNA3.1(+) FLAG-tagged HNRNPH2 mutants	
R212K Forward	CCCTATGATAAGCCGGGGGCT
R212K/N Reverse	ACCTGGCCGCTGCATAGC
R212A Forward	TCCCTATGATGCGCCGGGGGCTGG
R212A Reverse	CCTGGCCGCTGCATAGCC
R212N Forward	CCCTATGATAATCCGGGGGCTGGCAG
For Kapβ2 mutant	
W373A Forward	GGCGATACAATTTCAGACGCGAATCTAAGAAAATGTTCTGCTG
W373A Reverse	CAGCAGAACATTTTCTTAGATTCGCGTCTGAAATTGTATCGCC

References

1. Cansizoglu, A.E., Lee, B.J., Zhang, Z.C., Fontoura, B.M., and Chook, Y.M. (2007). Structure-based design of a pathway-specific nuclear import inhibitor. Nat Struct Mol Biol *14*, 452-454. 10.1038/nsmb1229.